*nanomaterials*

MDPI

*Article*

# N-Doped Honeycomb-like Ag@N-$Ti_3C_2T_x$ Foam for Electromagnetic Interference Shielding

**Xiaohan Wang [1], Fan Zhang [1,2], Feiyue Hu [1], Yaya Li [1,*], Yongqiang Chen [1], Hailong Wang [1], Zhiyu Min [3] and Rui Zhang [1,3]**

[1] School of Material Science and Engineering, Zhengzhou University, Zhengzhou 450001, China
[2] Henan Vocational College of Information and Statistics, Zhengzhou 450008, China
[3] School of Material Science and Engineering, Luoyang Institute of Science and Technology, Luoyang 471026, China
* Correspondence: lyzzu06@126.com

**Abstract:** To solve the pollution problem of electromagnetic waves, new electromagnetic shielding materials should meet the requirements of being lightweight with high electrical conductivity. In this work, the combination of silver (Ag) nanoparticles and nitrogen doping (N-doping) was expected to tune the electromagnetic and physical properties of $Ti_3C_2T_x$ MXene, and the Ag@N-$Ti_3C_2T_x$ composites were fabricated through the hydrothermal reactions. The nitrogen doped (N-doped) Ag@$Ti_3C_2T_x$ composites showed a hollow structure with a pore size of 5 µm. The influence of N-doped degrees on the electromagnetic interference (EMI) shielding performance was investigated over 8–18 GHz. Therefore, the controlled N-doping composites exhibited reflection-based EMI shielding performance due to the electrical conductivity and the special three-dimensional (3D) honeycomb-like structure. The achieved average EMI shielding values were 52.38 dB at the X-band and 72.72 dB at the $K_u$-band. Overall, the Ag@N-$Ti_3C_2T_x$ foam, due to its special 3D honeycomb-like structure, not only meets the characteristics of light weight, but also exhibits ultra-high-efficiency EMI shielding performance, revealing great prospects in the application of electromagnetic wave shielding field.

**Keywords:** nitrogen doping; Ag@N-$Ti_3C_2T_x$ composites; honeycomb-like structure; electromagnetic interference; multi-reflections



**Citation:** Wang, X.; Zhang, F.; Hu, F.; Li, Y.; Chen, Y.; Wang, H.; Min, Z.; Zhang, R. N-Doped Honeycomb-like Ag@N-$Ti_3C_2T_x$ Foam for Electromagnetic Interference Shielding. *Nanomaterials* **2022**, *12*, 2967. https://doi.org/10.3390/nano12172967

Academic Editor: Patrick Fiorenza

Received: 1 August 2022
Accepted: 24 August 2022
Published: 27 August 2022



## 1. Introduction

The development of telecommunication and portable electronic devices plays an important role in civilian and military applications; on the other hand, it has also been issued to cause serious electromagnetic interference problems. It may even threaten the human health. Hence, it is an urgent task to explore lightweight, efficient and environmentally friendly electromagnetic interference shielding materials to solve this kind of problem [1–4].

Traditionally, the efficient electromagnetic interference (EMI) shielding materials are made with intrinsic high electric conductivity or magnetics. Zeng et al. [5] synthesized Ni@carbon nanotubes (CNTs) in situ by the solvothermal method, and subsequently obtained PVDF/CNTs/Ni@CNTs composite films by solution casting and compression molding, which exhibited 51.4 dB of electromagnetic shielding performance. Younes et al. [6] coated carbon nanostructured (CNS) mats with $Fe_3O_4$ particles and explored its effect on electromagnetic shielding performance. Adding $Fe_3O_4$ to CNS mats, the electromagnetic shielding performance increased from 46.09 dB to 60.29 dB. However, due to the high density of metal and the shortcomings of easy agglomeration of carbon nanotubes, it does not meet the requirements for new electromagnetic shielding materials. Compared with traditional electromagnetic shielding materials, such as metals and carbon nanotubes, $Ti_3C_2T_x$ shows great prospects for EMI applications owing to its super high intrinsic electrical conductivity and chemically tunable properties. The EMI shielding performance of $Ti_3C_2T_x$

was first reported by Yury et al. [7] in 2016. They found that pure $Ti_3C_2T_x$ film exhibited EMI effectiveness of 92 dB in the range of 8.2–12.4 GHz. The 60 wt% $Ti_3C_2T_x$/paraffin composites presented the EMI shielding performance of 39.1 dB [8]. However, the application of $Ti_3C_2T_x$ in the field of electromagnetic shielding is often limited by the self-stacking effect. By fabricating the lamellar structure into a 3D structure, the self-stacking effect can be improved. Meanwhile, the transmission path of electromagnetic waves in the porous network can be increased, thus enhancing the electromagnetic wave loss [9]. When Zhang et al. [10] transferred the MXene film into MXene foam through the hydrazine-induced foaming method, the EMI shielding performance was improved from 53 dB to 70 dB. The increasing EMI shielding values were due to the high attenuation efficient of the electromagnetic wave in the three-dimensional cellular MXene foam. Wu et al. [11] prepared lightweight MXene/sodium alginate (SA) aerogel and obtained an EMI shielding performance of 70.5 dB.

These findings have prompted the exploration of MXene 3D structured composites to further enhance the intrinsic EMI shielding performance of MXene through building 3D microporous structures [12]. Based on previous work, 3D MXene based composites cannot only improve the electromagnetic shielding performance but also exhibit a good mechanical properties and high stability [13]. For example, the EMI shielding performance of 3D MXene/reduced graphene oxide (rGO)/polyurethane containing Diels-Alder bounds (PUDA) composite hardly changed after 5000 bending cycles [14]. MXene/AgNWs/Epoxy aerogel material obtained an EMI shielding performance of 94.1 dB and exhibited excellent thermal conductivity [15].

Recently, researchers reported that increasing the electrical conductivity of MXene through nitrogen doping could advance the electromagnetic absorption performance [16]. For example, a specific capacitance of $Ti_3C_2T_x$ (201 F/g) could be increased by nitrogen doping to 340 F/g [16]. Li et al. [17] obtained −59.20 dB absorption performance of N-doped $Ti_3C_2T_x$ at 10.56 GHz by $N_2$ plasma treatment method on $Ti_3C_2T_x$. Since the absorption loss is essential to the electromagnetic shielding performance, we intended to explore the electromagnetic shielding performance of N-doped 3D MXene based composites.

Inspired by these studies and based on our previous work [18,19], we employed a facile and stable route to fabricate a honeycomb-like N-doped Ag@$Ti_3C_2T_x$ foam. While not destroying its microscopic morphology, high electrical conductivity can also be obtained and, at the same time, it can meet the characteristic of light weight. The uniform distribution of Ag particles and successful doping of nitrogen could significantly increase the conductivity of $Ti_3C_2T_x$ MXene. Meanwhile, the constructed 3D cellular structure contributes to multiple reflections of electromagnetic wave in the inside channels. In terms of these effects, 3D Ag@N-$Ti_3C_2T_x$ foam exhibited an improved electromagnetic shielding property (72.72 dB at the $K_u$-band). This provides a new prospect for the development of advanced EMI shielding materials.

## 2. Experimental

### *2.1. Materials*

The materials used in this work were listed in Table 1. All of them were used without further purification.

**Table 1.** List of materials used in this work.

| Materials | Purity/Grain Size | Manufacturers |
|---|---|---|
| $Ti_3AlC_2$ MAX | ≥99% | 11 Technology Co., Ltd. |
| Hydrochloric acid (HCl) | 36–38 wt% | Aladdin Biochemical Technology Co., Ltd. |
| Lithium fluoride (LiF) | ≥99% | Macklin Biochemical Co., Ltd. |
| Polymethyl methacrylate (PMMA) | 5 μm | Dongguan Kemai New Material Co., Ltd. |
| Ethanol | analytical reagent | Aladdin Biochemical Technology Co., Ltd. |
| Silver nitrate ($AgNO_3$) | ≥99.8% | Sinopharm Chemical Reagent Co. Ltd. |
| Sodium hydroxide (NaOH) | ≥96% | Macklin Biochemical Co., Ltd. |
| Ammonia ($N_2H_4{\cdot}H_2O$) | ≥98% | Aladdin Biochemical Technology Co., Ltd. |

### *2.2. Synthesis of Honeycomb-like Ag@$Ti_3C_2T_x$ Composites*

$Ti_3C_2T_x$ MXene suspension was prepared using the etching method as previous reported [20]. In the process of preparing honeycomb-structured Ag@$Ti_3C_2T_x$ composites, the $Ti_3C_2T_x$/PMMA pellets were first fabricated by adding 0.04 g of PMMA (5 μm) into a 40-mL $Ti_3C_2T_x$ suspension (1 mg/mL) and stirring for 1 h at room temperature. Subsequently, 0.1 M NaOH was added to the mixture until the pH value was 11. Then, 20 mL of $AgNO_3$ solution (1.8 mM) was gradually added and stirred for 30 min. Next, the mixture was heated in a microwave (200 W) for 1 min. Subsequently, the mixture was cooled at room temperature, washed and filtered through a microporous monolayer membrane (Celgard 3501, 11 Technology Co. Ltd. Changchun). Finally, to remove the PMMA template, the composite membrane was annealed at 400 °C for 0.5 h in an argon atmosphere, and the self-supporting honeycomb-structured Ag@$Ti_3C_2T_x$ composites were obtained [19].

### *2.3. Synthesis of 3D Honeycomb-like Ag@N-$Ti_3C_2T_x$ Foam*

To investigate to effect of nitration degree on the physical property of MXene, the as-prepared honeycomb Ag@$Ti_3C_2T_x$ samples were immersed into 40 mL of hydrazine hydrate in an oil bath at 75 °C and stirred for 0 h, 12 h, 18 h and 24 h, respectively. During this process, hydrazine hydrate decomposed into $NH_3$ that would replace the functional groups on the surface of Ag@$Ti_3C_2T_x$. The obtained suspension was centrifuged at 5000 rpm for 5 min, and this process was repeated three times. The final products of Ag@N-$Ti_3C_2T_x$ were obtained by vacuum filtration and drying.

### *2.4. Characterization*

The crystal structure of Ag@N-$Ti_3C_2T_x$ composites was characterized using X-ray diffraction (XRD) coupled with Cu-Kα radiation (λ = 0.15418 nm). The scanning electron microscopy (SEM, JSM-7200F, JEOL, Tokyo) and transmission electron microscope (TEM, FEI Talos F200X, Waltham, America) were used to observe the microscopic morphologies and structures of samples. The surface chemical composition and valence states were measured using a X-ray photoelectron spectroscopy (XPS) spectrometer (Thermo Scientific Escalab 250Xi, Waltham, America). The conductivity of the composites was measured by a four-probe tester (RTS-8).

The paraffin-based Ag@N-$Ti_3C_2T_x$ composites with a mass fraction of 50% were prepared for the evaluation of their EMI shielding performance. They were pressed into a ring shape with an inner distance of 3.04 mm and an outer diameter of 7.00 mm. The EMI shielding performance was calculated using the scattering parameters tested by the Vector network analyzer (MS46322B, Anli Co., Ltd., Kanagawa, Japan) at X-band (8–12 GHz) and $K_u$-band (12–18 GHz). All the formulas used for calculation of the EMI shielding performance could be found in the supporting information [21].

## 3. Results and Discussion

The fabrication process of the 3D honeycomb-like Ag@N-$Ti_3C_2T_x$ foam is shown in Figure 1. Based on our previous work [18,19], the prepared honeycomb-like Ag@$Ti_3C_2T_x$ composites were further nitrogen doped in an oil bath with hydrazine hydrate as a nitrogen source. During this process, hydrazine hydrate decomposed into $NH_3$ that would replace the functional groups on the surface of Ag@$Ti_3C_2T_x$, and the Ag@N-$Ti_3C_2T_x$ foam was successfully prepared.

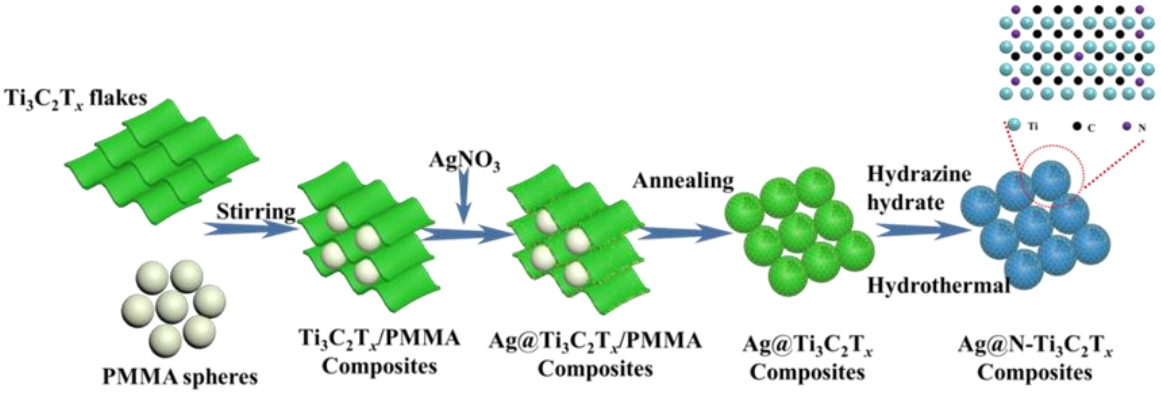


**Figure 1.** Schematic diagram of the preparation process of Ag@N-$Ti_3C_2T_x$ composites with honeycomb-like structure.

The XRD patterns of the prepared composites are shown in Figure 2a. The results showed that the (002) characteristic peak of $Ti_3C_2T_x$ was slightly left shifted from 6.42° to 5.23°. In the N-doped treatment of $Ti_3C_2T_x$ was further left shifted [16]. For the Ag@N-$Ti_3C_2T_x$ composites, the peak at 38° corresponds to the (111) crystal plane of fcc Ag. The surface chemical information was recorded in the XPS spectra of Figure 2b. As shown in the survey spectra, we could detect the elemental signals of F, Ti, O, C, Ag and N from the Ag@N–$Ti_3C_2T_x$ composites. Compared to pure $Ti_3C_2T_x$, the characteristic peak of N 1s at around 400 eV appears after the N-doped treatment. The reason for the appearance of N-$Ti_3C_2T_x$ is that hydrazine hydrate decomposes to produce $NH_3$, and the functional groups on the surface of $Ti_3C_2T_x$ react with $NH_3$ or are replaced. Thus, during the doping process, part of the $NH_3$ is attached to the surface of $Ti_3C_2T_x$ to form the N-$Ti_3C_2T_x$. The signal of N 1s from the N-doped honeycomb-like Ag@N-$Ti_3C_2T_x$ is weaker due to the presence of the Ag peak at 370 eV. The above results demonstrate the successful N-doping and preparation of honeycomb-like structured Ag@N-$Ti_3C_2T_x$ composites.

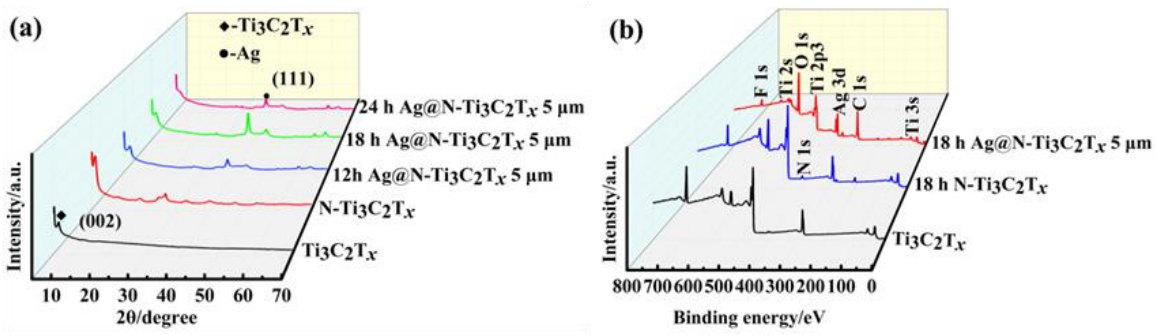


**Figure 2.** (**a**) XRD patterns and (**b**) XPS survey of $Ti_3C_2T_x$, N-$Ti_3C_2T_x$ and Ag@N-$Ti_3C_2T_x$ composites.

The high-resolution XPS spectra of Ti 2p, C 1s, O 1s, N 1s and Ag 3d are given in Figure 3. With the N-doping, it shows Ti-N bonds at the binding energies of 456 eV and 462 eV (Figure 3a) [16]. In Figure 3b, the peaks centered at 282 eV, 283 eV, 285 eV, 287 eV and 289 eV, corresponding to C-Ti-$T_x$, C-C, C-N, C-O and C=O, respectively [22]. The deconvoluted peaks of the O 1s at 530 eV, 531 eV, 532 eV and 535 eV are assigned to Ti-O-Ti, Ti-OH, O-N and -COO, respectively (Figure 3c). It can be seen that after N-doping, there were the C-N and O-N peaks [23], and the five deconvoluted peaks at 396.8 eV, 398.5 eV, 399.6 eV, 401.2 eV and 402.4 eV in the N 1s spectrum are assigned to N-Ti, pyridine-N, C-NH, C-$NH_2$ and oxidized-N, respectively (Figure 3d). The above analyses further indicate the successful doping of N in $Ti_3C_2T_x$ foam. Moreover, the high resolution of Ag 3d spectrum is displayed in Figure 3e. Compared to the N-$Ti_3C_2T_x$ composites (Figure S1), the two peaks

at the binding energies of 368 eV and 374 eV, linked to the formation of Ag° $3d_{3/2}$ and Ag° $3d_{5/2}$, respectively, which further confirmed that the Ag particles exist in the composites.

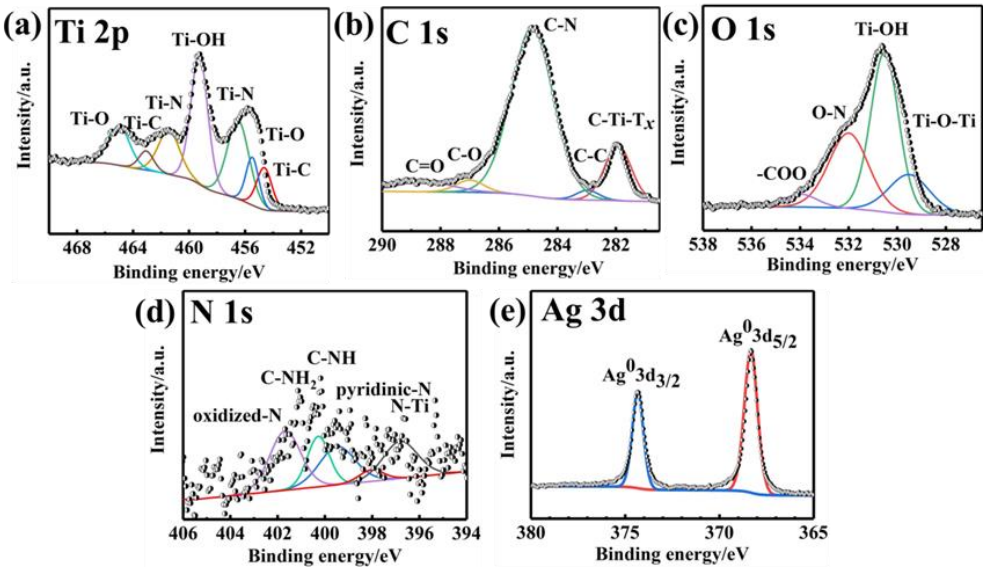


**Figure 3.** High-resolution XPS spectra of Ti 2p (**a**), C 1s (**b**), O 1s (**c**), N 1s (**d**) and Ag 3d (**e**) of Ag@N-$Ti_3C_2T_x$ composites.

The morphologies of N-$Ti_3C_2T_x$ lamellae and honeycomb-like Ag@N-$Ti_3C_2T_x$ foam were characterized by SEM, as shown in Figure 4a–e. There are wrinkles in the N-$Ti_3C_2T_x$, which is due to the lattice distortion caused by N-doping in the pristine $Ti_3C_2T_x$ layer [24]. The prepared honeycomb-like Ag@$Ti_3C_2T_x$ was nitrided in hydrazine hydrate to obtain honeycomb-like Ag@N-$Ti_3C_2T_x$ foam, and the honeycomb-like structure was retained even after N-doping. The measured pore diameter of Ag@N-$Ti_3C_2T_x$ composites was about 4 µm, and the diameter of an N-$Ti_3C_2T_x$ thin shell was about 10 nm (Figure 4b–e).

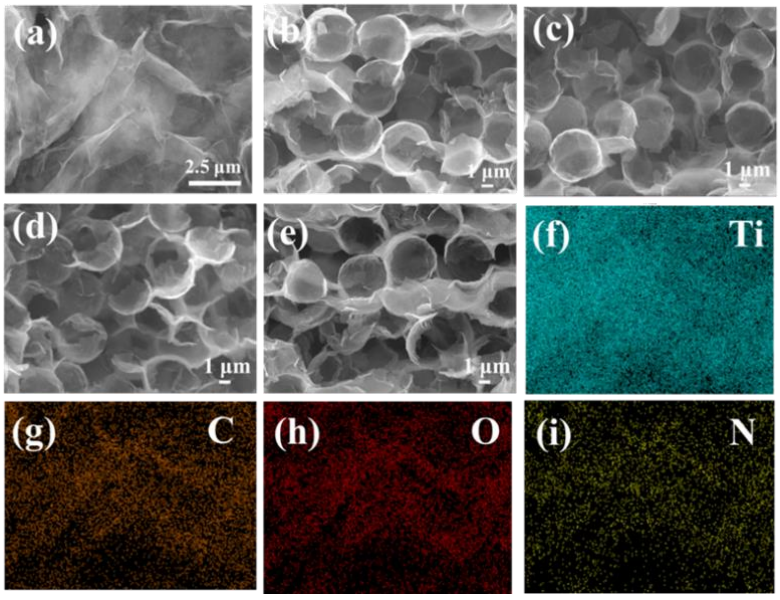


**Figure 4.** SEM images of (**a**) nitrogen doping $Ti_3C_2T_x$, (**b**) Ag@$Ti_3C_2T_x$ foam, (**c**) 12h Ag@N-$Ti_3C_2T_x$ foam nitriding for 12 h, (**d**) Ag@N-$Ti_3C_2T_x$ foam nitriding for 12 h and (**e**) Ag@N-$Ti_3C_2T_x$ foam nitriding for 12 h. (**f–i**) EDS mappings of Ti, C, O and N elements, respectively.

To further observe the elemental distribution in the samples, an energy spectrum surface scan of N-$Ti_3C_2T_x$ was performed. As shown in Figure 4f–i, the EDS mapping confirmed the uniform distribution of Ti, C, O and N elements in the N-$Ti_3C_2T_x$ composite, which indicates the successful doping of N elements as well.

The microstructure of N-$Ti_3C_2T_x$ and Ag@N-$Ti_3C_2T_x$ foam was further characterized by TEM. As shown in Figure 5a, the N-$Ti_3C_2T_x$ retains the flake-like structure of two-dimensional materials. The high-resolution TEM (HRTEM) image (Figure 5b) of the N-$Ti_3C_2T_x$ composites showed the corresponding lattice fringes from (006) of $Ti_3C_2T_x$ [25]. The SAED diagram (Figure 5c) confirms the hexagonal structure of parent $Ti_3C_2T_x$ MXene phase was maintained in the N-$Ti_3C_2T_x$. In Figure 5d, the original honeycomb-like structure had not collapsed even after being N-doped, and the Ag nanoparticles were closely attached to the $Ti_3C_2T_x$ shell (Figure 5d). The HRTEM image (Figure 5e) presents the corresponding lattice fringes of (111) of Ag and (006) of N-$Ti_3C_2T_x$. Figure 5f presents a variety of diffraction rings, confirming that the polycrystalline phase at the interface of the Ag and $Ti_3C_2T_x$ and the spacing of diffraction rings correspond to the (111) of Ag and (100) (110) of $Ti_3C_2T_x$, respectively.

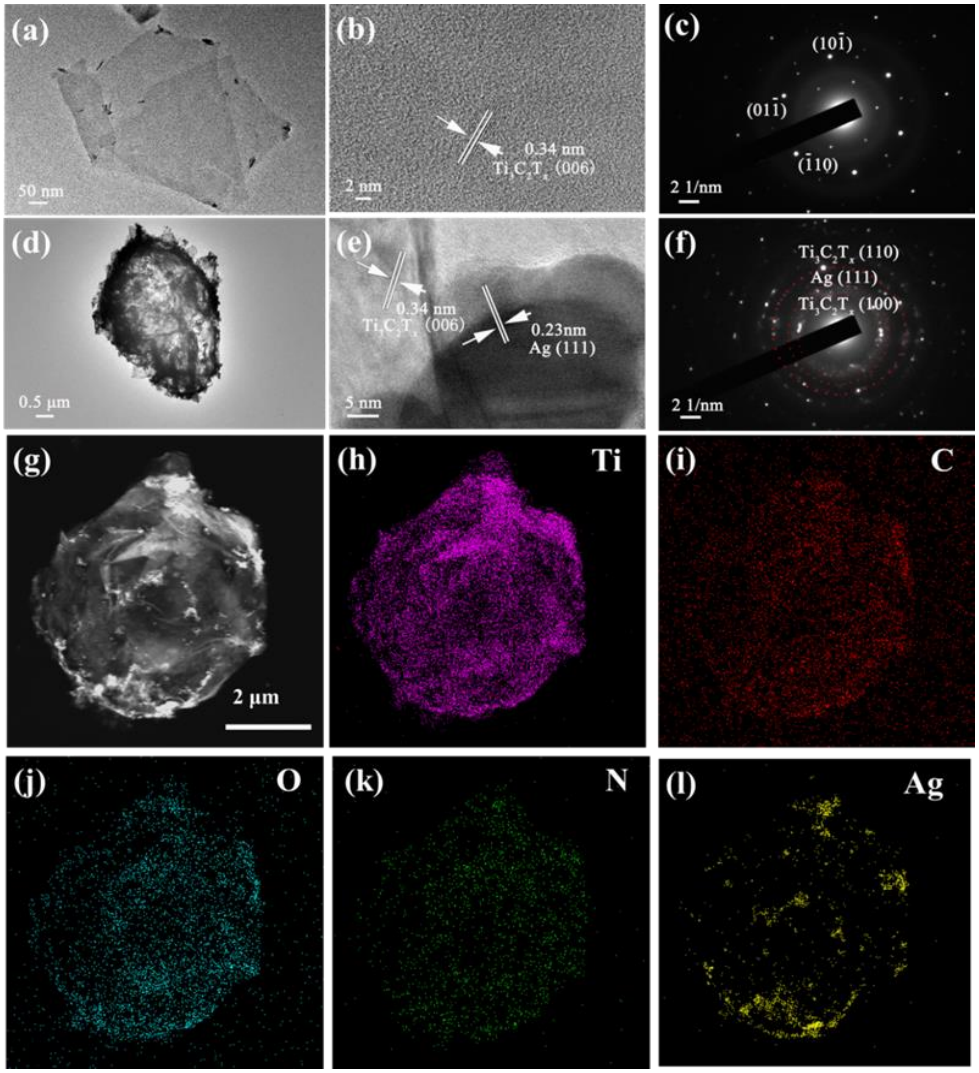


**Figure 5.** TEM image of (**a**) N-$Ti_3C_2T_x$ flakes, (**b**) HRTEM image of N-$Ti_3C_2T_x$ flakes, (**c**) SAED patterns of N-$Ti_3C_2T_x$ flakes, (**d**) TEM image of Ag@N-$Ti_3C_2T_x$ 5 μm, (**e**) HRTEM image of Ag and $Ti_3C_2T_x$ and (**f**) SAED patterns of Ag and $Ti_3C_2T_x$. (**g**) TEM image of Ag@N-$Ti_3C_2T_x$, (**h–l**) EDS mappings of Ti, C, O, N and Ag elements.

The elemental distribution on the surface of the prepared honeycomb-like structured Ag@N-$Ti_3C_2T_x$ 5 μm was shown in Figure 5h–l. The EDS pattern confirms the coexistence of Ti, C, O, N and Ag components in Ag@N-$Ti_3C_2T_x$ 5 μm composites, and the distribution of each element is relatively uniform, which further confirms the N doping in Ag@N-$Ti_3C_2T_x$ composites.

As described in the introduction, the conductivity of materials is crucial to the EMI shielding performance. We measured the electrical conductivity of the $Ti_3C_2T_x$, N-$Ti_3C_2T_x$ and Ag@N-$Ti_3C_2T_x$ with N-doping treated at varying hours (Figure 6). The N-doped $Ti_3C_2T_x$ has an electrical conductivity of 350 S/cm, which is about 1.7 times higher than that of pure $Ti_3C_2T_x$. In the presence of silver particles, the electrical conductivity of the honeycomb-like Ag@$Ti_3C_2T_x$ composites was 500 S/cm. As nitriding Ag@$Ti_3C_2T_x$ composites for 12 h, 18 h and 24 h, the electrical conductivity of the honeycomb-like Ag@N-$Ti_3C_2T_x$ composites was 520, 570 and 540 S/cm, respectively. This is mainly due to the great conductivity of sliver and the electron-giving effect of element N [26]. However, the silver effect was much more significant than the nitrogen doping effect. Moreover, as extra N doped into $Ti_3C_2T_x$, the increasing internal free electron concentrations indeed increase the conductivity of $Ti_3C_2T_x$ nanosheets [27], the over doping of nitrogen may make the $Ti_3C_2T_x$ oxidized and then generate $TiO_2$.

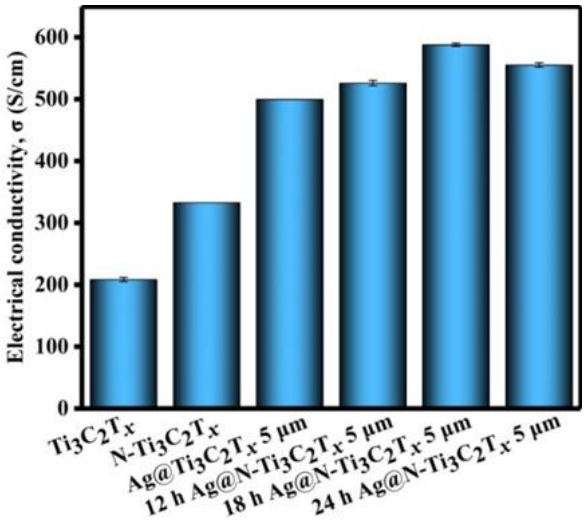


**Figure 6.** Electrical conductivity of $Ti_3C_2T_x$, N-$Ti_3C_2T_x$ and Ag@N-$Ti_3C_2T_x$ composites. The error bars were from five measurements.

The frequency dependent EMI shielding performance of the Ag@N-$Ti_3C_2T_x$ composites was shown in Figure 7a. The average EMI SE total of pure $Ti_3C_2T_x$, N-$Ti_3C_2T_x$ and honeycomb-like structured Ag@$Ti_3C_2T_x$ 5 μm at the X-band was 23.50 dB, 30.54 dB and 51.15 dB, respectively, while at the $K_u$-band, the values were 30.33 dB, 31.97 dB and 56.64 dB, respectively. With the N-doping treatment at 18 h, the average EMI SE total of the Ag@N-$Ti_3C_2T_x$ 5 μm honeycomb-like was 52.38 dB over the X-band and 72.72 dB over the $K_u$-band, which was higher than other samples in the frequency range of 10–18 GHz (Figure S2b). In addition, its reflectivity was the lowest in the $K_u$-band compared to other absorbers (Figure S2a). This phenomenon may be due to the N-doping and the electric conductivity.

In addition, at 12 GHz the SE totals of $Ti_3C_2T_x$, N-$Ti_3C_2T_x$ and 18 h Ag@N-$Ti_3C_2T_x$ 5 μm were 26.41 dB, 31.27 dB and 60.10 dB, respectively (Figure 7c), while at 18 GHz the SE total values of $Ti_3C_2T_x$, N-$Ti_3C_2T_x$ and 18 h Ag@N-$Ti_3C_2T_x$ were 29.96 dB, 33.91 dB and 75.27 dB, respectively (Figure 7d). Overall, the 18 h Ag@N-$Ti_3C_2T_x$ 5 μm composites exhibit the best EMI shielding performance with an average EMI SE total of 64.58 dB. The improvement in absorption loss has significantly contribution to $SE_T$ with a negligible improvement in reflection loss.

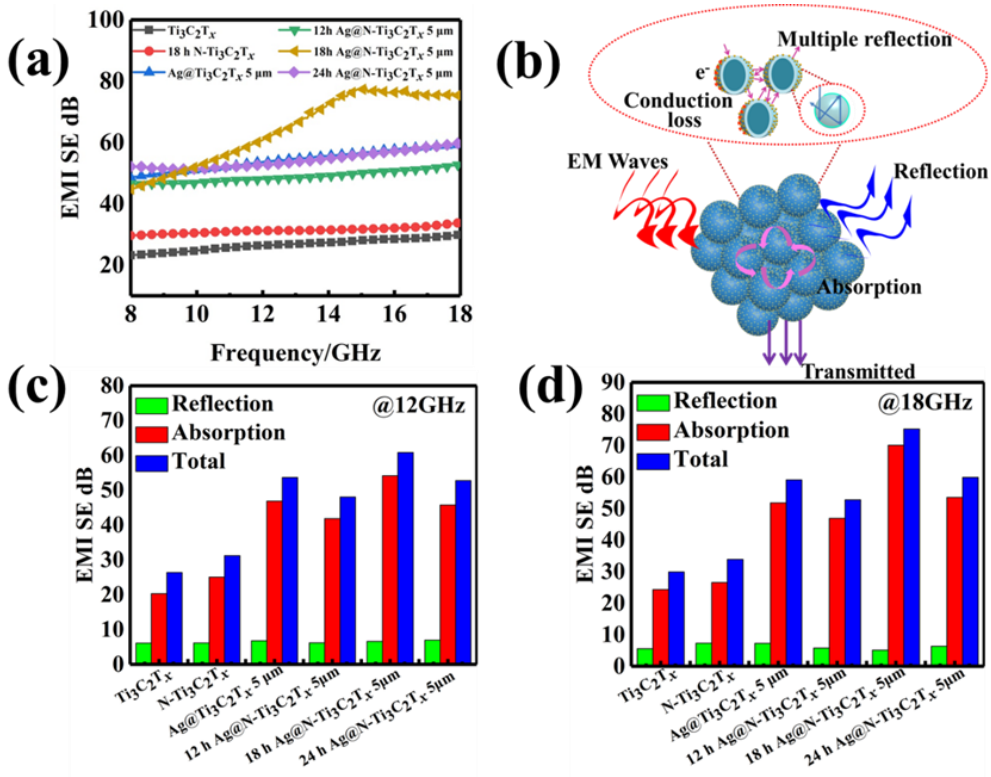


**Figure 7.** (**a**) EMI SE curve; (**b**) EMI shielding mechanism diagram of Ag@N-$Ti_3C_2T_x$ honeycomb structure; $SE_R$, $SE_A$ and $SE_T$ of the composites at 12 GHz (**c**) and at 18 GHz (**d**).

The electromagnetic shielding mechanisms of the honeycomb-like Ag@N-$Ti_3C_2T_x$ composite are summarized in Figure 7b. As fabricating the two-dimensional $Ti_3C_2T_x$ into a three-dimensional honeycomb-like structure, the propagation paths of electromagnetic waves diameter increase [28]. The transmissivity of pure $Ti_3C_2T_x$ was obviously decreased (Figure S2c). The multiple reflections of electromagnetic waves occurring in the honeycomb-like foam thus improve the electromagnetic shielding performance of Ag@N-$Ti_3C_2T_x$ composites [29]. Moreover, the special honeycomb-like structure provides high specific surface area. The measured values for N-$Ti_3C_2T_x$ and Ag@N-$Ti_3C_2T_x$ are 49.89 and 67.47 $m^2/g$, respectively, and the Ag nanoparticles distributed at the interfaces could generate the interfacial polarization relaxation loss. The charges then accumulate at these interfaces, leading to a strong interfacial polarization effect. The other factor can be attributed to the conduction loss. The conduction loss is related to the conductivity of the material. The higher the conductivity, the greater the macroscopic current caused by the carriers (including the current caused by the change in the electric field and the eddy current caused by the change of the magnetic field), which is conducive to the conversion of electromagnetic energy into heat energy. Both the introduction of Ag particles and the N-doping increase the electrical conductivity of the MXene material [26,30,31]. The increasing conductivity makes the skin depth ($\delta = \left(\sqrt{\pi f \mu \sigma}\right)^{-1}$) become smaller, thus, the electromagnetic wave cannot penetrate the material, and then electromagnetic shielding performance can also be improved. Hydrazine hydrate provides a reducing environment as a nitrogen source to avoid oxidation. However, the long nitriding time would lead to the generation of $NH_3$ gas from hydrazine hydrate and cause the $Ti_3C_2T_x$ to be oxidized into $TiO_2$. The generation of $TiO_2$ will lead to a decrease in its own conductivity and affect the electromagnetic shielding performance of the material.

## 4. Conclusions

In this research, honeycomb-like Ag@N-$Ti_3C_2T_x$ with different degrees of nitridation was prepared by using hydrazine hydride nitridation. Even after N-doping, the Ag@N-

$Ti_3C_2T_x$ composite still retained its original honeycomb-like structure in the same size. In the nitridation for 18 h, the electrical conductivity of Ag@N-$Ti_3C_2T_x$ composites was 500 S/cm. The electromagnetic shielding performance was significantly improved by N-doping and the decoration of Ag particles. The average electromagnetic shielding performance was 52.38 dB, covering the whole X-band, and 72.72 dB over the Ku-band. The excellent electromagnetic shielding property of Ag@N-$Ti_3C_2T_x$ composites comes from its own conductivity loss, the interfacial polarization between Ag nanoparticles and the N-$Ti_3C_2T_x$ shell, the dipole polarization at the N dipole polarization at the defects, and multiple reflections and scatterings caused by the hollow honeycomb-like structure of the composite.

**Supplementary Materials:** Reference [21] is cited in the supplementary materials. The following supporting information can be downloaded at: https://www.mdpi.com/article/10.3390/nano12172967/s1, Figure S1: High-resolution XPS spectra of Ti 2p (a), C 1s (b), O 1s (c) and N 1s (d) of N-$Ti_3C_2T_x$ composites; Figure S2: The (a) reflectivity, (b) absorptivity and (c) transmittivity of $Ti_3C_2T_x$, N-$Ti_3C_2T_x$ and Ag@N-$Ti_3C_2T_x$ composites.

**Author Contributions:** Research concept and design: X.W.; Acquisition of data: X.W.; draft preparation, X.W.; Analysis and interpretation of data: X.W., Y.L.; Paper-review and editing: X.W., Y.L.; Final proofreading and approval of version for publication: F.Z., F.H., Y.L., Y.C., H.W., Z.M. and R.Z. All authors have read and agreed to the published version of the manuscript.

**Funding:** This research was funded by the National Natural Science Foundation of China (No. U2004177).

**Data Availability Statement:** Not Applicable.

**Acknowledgments:** The authors appreciate the support from the National Natural Science Foundation of China (No. U2004177), Outstanding Youth Funding in Henan Province (No. 212300410081).

**Conflicts of Interest:** The authors declare no conflict of interest.

## References

1. Du, Y.; Wang, X.; Dai, X.; Lu, W.; Tang, Y.; Kong, J. Ultraflexible, highly efficient electromagnetic interference shielding, and self-healable triboelectric nanogenerator based on $Ti_3C_2T_x$ MXene for self-powered wearable electronics. *J. Mater. Sci. Technol.* **2022**, *100*, 1–11. [CrossRef]
2. Du, H.; Zhang, Q.; Zhao, B.; Marken, F.; Gao, Q.; Lu, H.; Guan, L.; Wang, H.; Shao, G.; Xu, H.; et al. Novel hierarchical structure of $MoS_2/TiO_2/Ti_3C_2T_x$ composites for dramatically enhanced electromagnetic absorbing properties. *J. Adv. Ceram.* **2021**, *10*, 1042–1051. [CrossRef]
3. Song, L.; Zhang, F.; Chen, Y.; Guan, L.; Zhu, Y.; Chen, M.; Wang, H.; Putra, B.R.; Zhang, R.; Fan, B. Multifunctional SiC@$SiO_2$ Nanofiber Aerogel with Ultrabroadband Electromagnetic Wave Absorption. *Nano-Micro Lett.* **2022**, *14*, 152. [CrossRef] [PubMed]
4. Niu, H.; Tu, X.; Zhang, S.; Li, Y.; Wang, H.; Shao, G.; Zhang, R.; Li, H.; Zhao, B.; Fan, B. Engineered core-shell $SiO_2$@$Ti_3C_2T_x$ composites: Towards ultra-thin electromagnetic wave absorption materials. *Chem. Eng. J.* **2022**, *446*, 137260. [CrossRef]
5. Zeng, S.; Li, X.; Li, M.; Zheng, J.; Shiju, E.; Yang, W.; Zhao, B.; Guo, X.; Zhang, R. Flexible PVDF/CNTs/Ni@CNTs composite films possessing excellent electromagnetic interference shielding and mechanical properties under heat treatment. *Carbon* **2019**, *155*, 34–43. [CrossRef]
6. Younes, H.; Shoaib, N.; Rahman, M.M.; Abu Al-Rub, R.; Hong, H.; Christensen, G.; Chen, H.; Younes, A.B.; Al Ghaferi, A. Thin carbon nanostructure mat with high electromagnetic interference shielding performance. *Synth. Met.* **2019**, *253*, 48–56. [CrossRef]
7. Shahzad, F.; Alhabeb, M.; Hatter, C.B.; Anasori, B.; Man Hong, S.; Koo, C.M.; Gogotsi, Y. Electromagnetic interference shielding with 2D transition metal carbides (MXenes). *Science* **2016**, *353*, 1137–1140. [CrossRef]
8. Liu, X.; Wu, J.; He, J.; Zhang, L. Electromagnetic interference shielding effectiveness of titanium carbide sheets. *Mater. Lett.* **2017**, *205*, 261–263. [CrossRef]
9. Lu, Y.; Zhang, S.; He, M.; Wei, L.; Chen, Y.; Liu, R. 3D cross-linked graphene or/and MXene based nanomaterials for electromagnetic wave absorbing and shielding. *Carbon* **2021**, *178*, 413–435. [CrossRef]
10. Liu, J.; Zhang, H.-B.; Sun, R.; Liu, Y.; Liu, Z.; Zhou, A.; Yu, Z.-Z. Hydrophobic, Flexible, and Lightweight MXene Foams for High-Performance Electromagnetic-Interference Shielding. *Adv. Mater.* **2017**, *29*, 1702367. [CrossRef]
11. Wu, X.; Han, B.; Zhang, H.-B.; Xie, X.; Tu, T.; Zhang, Y.; Dai, Y.; Yang, R.; Yu, Z.-Z. Compressible, durable and conductive polydimethylsiloxane-coated MXene foams for high-performance electromagnetic interference shielding. *Chem. Eng. J.* **2020**, *381*, 122622. [CrossRef]
12. Li, X.; Yin, X.; Song, C.; Han, M.; Xu, H.; Duan, W.; Cheng, L.; Zhang, L. Self-Assembly Core-Shell Graphene-Bridged Hollow MXenes Spheres 3D Foam with Ultrahigh Specific EM Absorption Performance. *Adv. Funct. Mater.* **2018**, *28*, 1803938. [CrossRef]

13. Sambyal, P.; Iqbal, A.; Hong, J.; Kim, H.; Kim, M.K.; Hong, S.M.; Han, M.; Gogotsi, Y.; Koo, C.M. Ultralight and Mechanically Robust $Ti_3C_2T_x$ Hybrid Aerogel Reinforced by Carbon Nanotubes for Electromagnetic Interference Shielding. *ACS Appl. Mater. Inter.* **2019**, *11*, 38046–38054. [CrossRef] [PubMed]
14. Li, H.; Ru, X.; Song, Y.; Wang, H.; Yang, C.; Gong, L.; Liu, Z.; Zhang, Q.; Chen, Y. Flexible and self-healing 3D MXene/reduced graphene oxide/polyurethane composites for high-performance electromagnetic interference shielding. *Compos. Sci. Technol.* **2022**, *227*, 109602. [CrossRef]
15. Liu, H.; Huang, Z.; Chen, T.; Su, X.; Liu, Y.; Fu, R. Construction of 3D MXene/Silver nanowires aerogels reinforced polymer composites for extraordinary electromagnetic interference shielding and thermal conductivity. *Chem. Eng. J.* **2022**, *427*, 131540. [CrossRef]
16. Zhang, T.; Xiao, J.; Li, L.; Zhao, J.; Gao, H. A high-performance supercapacitor electrode based on freestanding N-doped $Ti_3C_2T_x$ film. *Ceram. Int.* **2020**, *46*, 21482–21488. [CrossRef]
17. Xu, W.; Li, S.; Zhang, W.; Ouyang, B.; Yu, W.; Zhou, Y. Nitrogen-Doped $Ti_3C_2T_x$ MXene Induced by Plasma Treatment with Enhanced Microwave Absorption Properties. *ACS Appl. Mater. Inter.* **2021**, *13*, 49242–49253. [CrossRef]
18. Wang, X.; Chen, Y.; Hu, F.; Zhang, S.; Fan, B.; Min, Z.; Zhang, R.; Zhao, B.; Wang, H.; Lu, H.; et al. Electromagnetic Interference Shielding Performance of Flexible, Hydrophobic Honeycomb-Structured Ag@$Ti_3C_2T_x$ Composites. *Adv. Electron. Mater.* **2022**, *8*, 2101028. [CrossRef]
19. Wang, X.; Bao, S.; Hu, F.; Shang, S.; Chen, Y.; Zhao, N.; Zhang, R.; Zhao, B.; Fan, B. The effect of honeycomb pore size on the electromagnetic interference shielding performance of multifunctional 3D honeycomb-like Ag/$Ti_3C_2T_x$ hybrid structures. *Ceram. Int.* **2022**, *48*, 16892–16900. [CrossRef]
20. Zhang, T.; Pan, L.; Tang, H.; Du, F.; Guo, Y.; Qiu, T.; Yang, J. Synthesis of two-dimensional $Ti_3C_2T_x$ MXene using HCl plus LiF etchant: Enhanced exfoliation and delamination. *J. Alloy. Compd.* **2017**, *695*, 818–826. [CrossRef]
21. Raagulan, K.; Braveenth, R.; Jang, H.J.; Seon Lee, Y.; Yang, C.M.; Mi Kim, B.; Moon, J.J.; Chai, K.Y. Electromagnetic Shielding by MXene-Graphene-PVDF Composite with Hydrophobic, Lightweight and Flexible Graphene Coated Fabric. *Materials* **2018**, *11*, 1803. [CrossRef] [PubMed]
22. Halim, J.; Cook, K.M.; Naguib, M.; Eklund, P.; Gogotsi, Y.; Rosen, J.; Barsoum, M.W. X-ray photoelectron spectroscopy of select multi-layered transition metal carbides (MXenes). *Appl. Surf. Sci.* **2016**, *362*, 406–417. [CrossRef]
23. Wang, X.; Fu, Q.; Wen, J.; Ma, X.; Zhu, C.; Zhang, X.; Qi, D. 3D $Ti_3C_2T_x$ aerogels with enhanced surface area for high performance supercapacitors. *Nanoscale* **2018**, *10*, 20828–20835. [CrossRef] [PubMed]
24. Li, W.; Lü, H.-Y.; Wu, X.-L.; Guan, H.; Wang, Y.-Y.; Wan, F.; Wang, G.; Yan, L.-Q.; Xie, H.-M.; Wang, R.-S. Electrochemical performance improvement of N-doped graphene as electrode materials for supercapacitors by optimizing the functional groups. *RSC Adv.* **2015**, *5*, 12583–12591. [CrossRef]
25. Yoon, Y.; Tiwari, A.P.; Lee, M.; Choi, M.; Song, W.; Im, J.; Zyung, T.; Jung, H.-K.; Lee, S.S.; Jeon, S.; et al. Enhanced electrocatalytic activity by chemical nitridation of two-dimensional titanium carbide MXene for hydrogen evolution. *J. Mater. Chem. A* **2018**, *6*, 20869–20877. [CrossRef]
26. Zhao, T.; Zhang, J.; Du, Z.; Liu, Y.; Zhou, G.; Wang, J. Dopamine-derived N-doped carbon decorated titanium carbide composite for enhanced supercapacitive performance. *Electrochim. Acta* **2017**, *254*, 308–319. [CrossRef]
27. Zhang, C.; Wang, L.; Lei, W.; Wu, Y.; Li, C.; Khan, M.A.; Ouyang, Y.; Jiao, X.; Ye, H.; Mutahir, S.; et al. Achieving quick charge/discharge rate of 3.0 V $s^{-1}$ by 2D titanium carbide (MXene) via N-doped carbon intercalation. *Mater. Lett.* **2019**, *234*, 21–25. [CrossRef]
28. Song, Y.; Yin, F.; Zhang, C.; Guo, W.; Han, L.; Yuan, Y. Three-Dimensional Ordered Mesoporous Carbon Spheres Modified with Ultrafine Zinc Oxide Nanoparticles for Enhanced Microwave Absorption Properties. *Nano-Micro Lett.* **2021**, *13*, 76.
29. Huang, L.; Li, J.; Li, Y.; He, X.; Yuan, Y. Lightweight and flexible hybrid film based on delicate design of electrospun nanofibers for high-performance electromagnetic interference shielding. *Nanoscale* **2019**, *11*, 8616–8625. [CrossRef]
30. Naguib, M.; Mashtalir, O.; Lukatskaya, M.R.; Dyatkin, B.; Zhang, C.; Presser, V.; Gogotsi, Y.; Barsoum, M.W. One-step synthesis of nanocrystalline transition metal oxides on thin sheets of disordered graphitic carbon by oxidation of MXenes. *Chem. Commun.* **2014**, *50*, 7420–7423.
31. Liao, Y.; Huang, Y.; Shu, D.; Zhong, Y.; Hao, J.; He, C.; Zhong, J.; Song, X. Three-dimensional nitrogen-doped graphene hydrogels prepared via hydrothermal synthesis as high-performance supercapacitor materials. *Electrochim. Acta* **2016**, *194*, 136–142.